Bayesian Comparison of Voice Coil Impedance Models for Dynamic Loudspeakers

R. Wesley Henderson[1,a)] and Paul M. Goggans[1,b)]

[1]*Department of Electrical Engineering, University of Mississippi, P.O. Box 1848, University, MS 38677*

[a)]Corresponding author: rwhender@go.olemiss.edu
[b)]goggans@olemiss.edu

Abstract. Loudspeaker design requires accurate models of driver voice coil impedance. This paper examines three model classes (standard, Leach, and van Maanen) from the audio literature and compares them using Bayesian model comparison via nested sampling. Data is generated from impedance measurements of two commercial loudspeaker drivers. We conclude that, for most design tasks involving these drivers, the van Maanen model with 3 lossy inductance groups is the most appropriate model.

INTRODUCTION

Loudspeaker system designers need accurate models of loudspeaker driver electrical impedance to produce high-quality speaker systems. The standard linear lumped-element circuit model can mostly describe a loudspeaker driver's impedance; however, the standard model fails to account for the exact shape of the impedance magnitude curve at frequencies higher than the low-frequency resonance peak. This discrepancy is caused by eddy current losses in the magnetic structure of the loudspeaker. Here we examine two model classes claimed to account for this loss. The first was described by Leach in 2002 [1] and includes a nonlinear, frequency-dependent lossy inductive component placed in series with the standard lumped element circuit model of the voice coil. The second was proposed by van Maanen and Zonneveld in 1994 [2], and it includes one or more elements also placed in series with the standard voice coil model, where each element consists of a linear resistor and linear inductor in parallel.

The loudspeaker design community generally does not use a rigorous model selection process. The designer chooses a model he or she thinks should work well (one of the three classes discussed here, or perhaps another), performs parameter estimation using the measured data, and as long as the fit is good to the eye, the process is finished. Our approach is novel and potentially useful, not only because it is Bayesian, but because it applies a quantitative model comparison framework in the first place. Using measured loudspeaker impedance data, we use nested sampling to compute the evidence for the standard linear voice coil model, the Leach nonlinear model, and the van Maanen model with several different combinations of lossy inductive elements.

DYNAMIC LOUDSPEAKER

Various textbooks explain how dynamic loudspeakers work, including Marshall Leach's *Introduction to Electroacoustics & Audio Amplifier Design* [3]. This section briefly summarizes the topic. A loudspeaker converts electrical signals into acoustical vibrations. In dynamic loudspeakers, a cylindrical voice coil carrying signal current interacts with a permanent magnet to induce motion in the diaphragm. Figure 1 depicts a cross-section of a typical dynamic loudspeaker.

Traditionally, the dynamic loudspeaker is modeled as a second-order mechanical system, consisting of components that can be grouped as masses, springs, and dashpots. The spider and (to a minor degree) the suspension comprise the spring component of the system, i.e., the part of the system that resists displacement. The voice coil, the diaphragm, the dust cap, and the unenclosed air moved by the diaphragm all contribute to the mass of the system, i.e., the part of the system that resists acceleration. Finally, the losses in the motion of the spider and in the movement

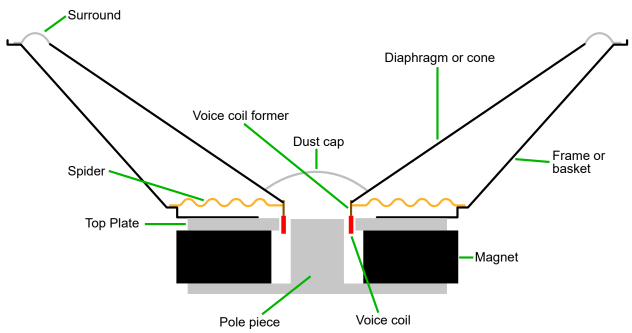

Figure 1. Loudspeaker cross-section illustration. Not to scale. [4]

Table 1. Second-order system parameters

Parameter	Description
K	spring constant due to the stiffness of the spider
M	mass due to the moving parts in the system: the voice coil, the diaphragm, the dust cap, and the unenclosed air moved by the diaphragm
D	damping constant due to the losses in the suspension elements and the air moved by the diaphragm
B	radial component of the magnetic flux density in the gap between the top plate and the pole piece
f_e	force applied to the cone by the voice coil current interacting with the magnetic field in the gap
l	total length of the wire the makes up the voice coil

of the air around the diaphragm make up the system's dashpot component and provide resistance to velocity. The system's driving force comes from the voice coil's interaction with the magnetic field due to the permanent magnet. The motion of this system can be described by a second-order linear differential equation with displacement variable x and voice coil current i,

$$M\frac{d^2x}{dt^2} + D\frac{dx}{dt} + Kx = f_e = Bli, \tag{1}$$

with parameters as shown in Table 1. Figure 2 (a) is a schematic diagram of this system.

Voice Coil Impedance

The voice coil is modeled as a single-loop circuit, as shown in Figure 2 (b). Parameters for this equivalent circuit are defined in Table 2.

Kirchhoff's voltage law (KVL) for the single loop circuit can be written as

$$v_T = iR_E + L\frac{di}{dt} + Bl\frac{dx}{dt}. \tag{2}$$

The Laplace transforms of (1) and (2) are given as

$$s^2MX + sDX + KX = BlI \tag{3}$$

$$R_EI + sLI + sBlX = V_T. \tag{4}$$

Evaluating the Laplace domain equations along the complex axis and some algebraic manipulation yield the following frequency domain expression for the impedance seen by the driving circuit:

$$Z(\omega) = \frac{V_T}{I} = R_E + j\omega L + \frac{j\omega(Bl)^2}{(K - \omega^2M) + j\omega D}. \tag{5}$$

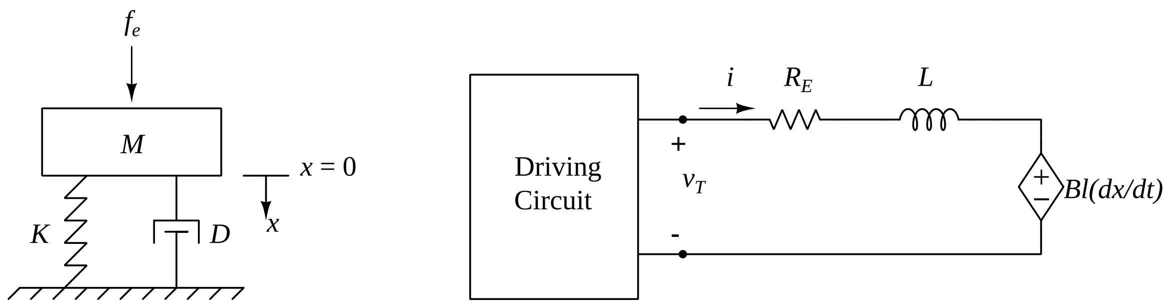

(a) Schematic diagram of a damped spring-mass system

(b) Driving circuit attached to voice coil equivalent circuit

Figure 2. Schematic diagrams for the loudspeaker's coupled equivalent systems

Table 2. Voice coil equivalent circuit parameters

Parameter	Description
v_T	terminal voltage at the voice coil input
R_E	DC resistance of the voice coil
L	inductance of the voice coil, potentially a nonlinear function

Defining the resonant frequency (ω_S), mechanical quality factor (Q_{MS}), and the difference between the impedance magnitude at the resonant frequency and at DC (R_{ES}) as

$$\omega_S \triangleq \sqrt{\frac{K}{M}},$$
$$Q_{MS} \triangleq \frac{1}{D}\sqrt{MK},$$
$$R_{ES} \triangleq \frac{(Bl)^2}{D},$$

the impedance can be rewritten in terms of these parameters as

$$Z(\omega) = R_E + j\omega L + R_{ES}\frac{j\,(1/Q_{MS})\,(\omega/\omega_s)}{1 - \left(\frac{\omega}{\omega_s}\right)^2 + j\,(1/Q_{MS})\,(\omega/\omega_s)}. \tag{6}$$

Voice Coil Impedance Models

We consider three models for the voice coil impedance. These models apply different functions to the inductance term ($j\omega L$) in (6), with one assuming that the inductance is real and constant, and others accounting for magnetic losses using a complex L that is a function of frequency. The impedance magnitude of inductive elements is greater at higher frequencies, so these models mostly differ in how they describe the high-frequency impedance. The inductance of the voice coil can have a small effect in the low-frequency regime as well, introducing a slight asymmetry about the resonant peak in the impedance curve, and the models that include lossy inductance terms better account for this asymmetry.

Standard model The simplest model uses a constant, frequency-independent value for L, so that the inductive component of the impedance is linear in frequency. This model assumes a lossless inductance, has five free parameters, and is given as

$$j\omega L(\omega) = j\omega L_E. \tag{7}$$

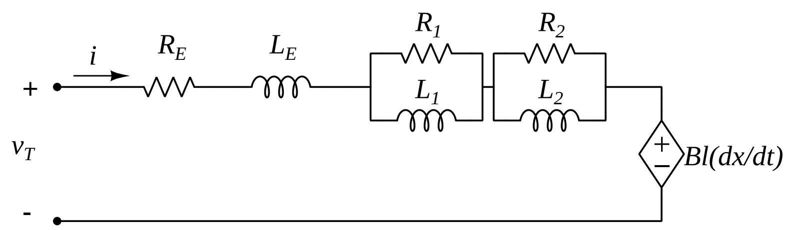

Figure 3. Voice coil equivalent circuit for the van Maanen model with two lossy inductance groups ($N = 2$)

Leach model The Leach model [1] replaces the constant, frequency-independent inductor value of the standard model with a two-parameter nonlinear function of frequency, yielding the expression,

$$j\omega L(\omega) = K(j\omega)^n. \tag{8}$$

The model attempts to account for magnetic losses, and it has six free parameters.

Van Maanen model The van Maanen model [2] describes the voice coil inductance as one or more groups in series, each group consisting of a resistor and linear inductor in parallel. The inductance term of the impedance expression is given as

$$j\omega L(\omega) = j\omega L_E + \sum_{n=1}^{N} \frac{R_n \omega^2 L_n^2}{R_n^2 + \omega^2 L_n^2} + j\frac{R_n^2 \omega L_n}{R_n^2 + \omega^2 L_n^2}. \tag{9}$$

Figure 3 shows one possible realization of the van Maanen model equivalent voice coil circuit, with $N = 2$. The van Maanen model describes a lossy inductance, and each additional lossy inductive group tends to improve the model's fit with the data. This model has $5 + 2N$ free parameters.

BAYESIAN INFERENCE FRAMEWORK

We use nested sampling to perform model comparison among the voice coil impedance models described in the previous section. This section describes the prior distributions, likelihood function, and model comparison process used.

Prior

Each model parameter is assigned a maximum-entropy prior distribution. For the DC voice coil resistance, we use a high-precision multimeter to perform an initial measurement of this value. There is some slight variation in this measurement over time, likely due to thermal noise, so the multimeter's built-in max-min function is used to observe the maximum and minimum values for R_E over about 300 measurements. These maximum and minimum values are used to assign a tight uniform prior distribution to R_E.

The drivers' datasheets provide design values for the other parameters common to each model, although imperfections in manufacturing lead to some unknown amount of variation. We interpret this state of knowledge as follows: we know the expected value of the parameters, and we know that each parameter is positive, but we do not know the prior variance for any of the parameters. Thus, we assign exponential prior distributions to each of these model parameters with means equal to the design values listed in the datasheets. Table 3 details the prior distribution constants for each of the model parameters.

For the Leach model, intuition suggests that the value of K is related to the value of L_E in the standard model. Assuming both the standard and Leach models agree at some angular frequency ω_0, the following relation is true: $j\omega_0 L_E = K(j\omega_0)^n$. Taking the magnitude of both sides, we have $\omega_0 L_E = K\omega_0^n$, and $K = L_E \omega_0^{1-n}$. Results from [1] suggest that n is usually around 0.5, and if we set ω_0 to a value that will allow the prior to cover the largest reasonable space, such as $2\pi 20$ krad/s, we have $K \approx 350 L_E$. This value is used as the mean for the exponential prior for K in Table 3.

Table 3. Parameter prior distributions for each of the two loudspeaker drivers tested

Parameter	Morel MW-166es	Morel UW-1058c
R_E	U(6.481511 Ω, 6.483864 Ω)	U(6.848636 Ω, 6.907280 Ω)
R_{ES}	Exp(λ = 29.578 Ω)	Exp(λ = 15.786 Ω)
Q_{MS}	Exp(λ = 2.79)	Exp(λ = 1.72)
ω_s	Exp($\lambda = 2\pi 46$ rad/s)	Exp($\lambda = 2\pi 26$ rad/s)
L_E	Exp(λ = 610 μH)	Exp(λ = 1.33 mH)
K	Exp(λ = 0.2135)	Exp(λ = 0.4655)
n	U(0, 1)	U(0, 1)
R_n and L_n	See "Prior" subsection	

For the van Maanen model, dependencies among the R_n and L_n parameters lead us to assign a more complex prior distribution. With (9) inserted into (6), two asymptotic expressions can be written. Let $\omega_n = R_n/L_n$. For $\omega \gg \max_n \omega_n$ and $\omega \gg \omega_S$, we have

$$Z(\omega) \approx R_E + \sum_{n=1}^{N} R_n + j\omega L_E. \tag{10}$$

For $\omega \ll \min_n \omega_n$ and $\omega \ll \omega_S$, we have

$$Z(\omega) \approx R_E + j\omega \left[L_E + \sum_{n=1}^{N} L_n \right] \tag{11}$$

Define the following:

$$R_t \triangleq \sum_{n=1}^{N} R_n = \mathrm{Re}\left\{Z\left(\omega_L\right)\right\} - R_E, \tag{12}$$

$$L_t \triangleq \sum_{n=1}^{N} L_n = \mathrm{Im}\left\{Z\left(\omega_0\right)\right\}/\omega_0 - L_E. \tag{13}$$

We have no further prior information about the lossy inductive components of the model, so we define a joint uniform prior for the sets of R_n and L_n conditioned on the proposition that those values sum to R_t and L_t. We have

$$p\left(R_1, \cdots, R_N \left| \sum_{n=1}^{N} R_n = R_t, I \right.\right) = k_1, \tag{14}$$

$$p\left(L_1, \cdots, L_N \left| \sum_{n=1}^{N} L_n = L_t, I \right.\right) = k_2, \tag{15}$$

where k_1 and k_2 are constants such that the prior distributions are normalized. Additionally, we assume that our data is such that the asymptotic expressions (12) and (13) give approximations for R_t and L_t, and we express this uncertainty by assigning R_t and L_t exponential priors with means defined by (12) and (13). In practice, these dependent uniform priors are incorporated into the computational inference using a reparameterization technique described by Goggans, et al. [5]

Likelihood

The principle of maximum entropy and a lack of knowledge of the error variance lead us to use an unnormalized Student's-t distribution as the likelihood function for each model. For parameter vector $\mathbf{\Theta}$, I measured complex

Figure 4. Tested drivers suspended in low-frequency anechoic chamber. Left: Morel MW-166es woofer, right: Morel UW-1058c subwoofer

impedance values $d_{\mathrm{real}}(\omega_i) + jd_{\mathrm{imag}}(\omega_i)$, and mock data $Z_{VC}(\mathbf{\Theta})$, the likelihood function is given as

$$\mathcal{L}(\mathbf{\Theta}) = -I \log \left\{ \sum_{i=1}^{I} \left(d_{\mathrm{real}}(\omega_i) - \mathrm{Re}\left[Z_{VC}(\omega_i; \mathbf{\Theta})\right]\right)^2 + \left(d_{\mathrm{imag}}(\omega_i) - \mathrm{Im}\left[Z_{VC}(\omega_i; \mathbf{\Theta})\right]\right)^2 \right\}. \tag{16}$$

Model comparison

We use a traditional nested sampling [6] implementation to estimate a log-evidence value for each model using two separate sets of data, corresponding to two different loudspeaker drivers. We do not assume that we have an exhaustive set of models, so we use the log-evidence values to compute the log-odds for each model against the standard model. Our nested sampling implementation uses 50 live samples and a one-dimension-at-a-time random walk algorithm to perform constrained prior exploration. The random walk algorithm takes 200 full steps per likelihood constraint. A full step consists of varying each parameter in turn by a Gaussian variate with a scale that increases or decreases throughout the run depending on the acceptance rate. The order of the parameter perturbations is shuffled at each step.

MEASUREMENT AND RESULTS

We performed impedance measurements on two commercially available loudspeaker drivers: the Morel MW-166es woofer (Figure 4, left) and the Morel UW-1058c subwoofer (Figure 4, right). We tested each driver while it was isolated in a low-frequency anechoic chamber using a Digilent Analog Discovery board, a custom impedance measurement jig, and an Audiosource monoblock amplifier.

Figure 5 shows the real and imaginary measured data and maximum a-posteriori (MAP) model mock data for each of the tested drivers. Figure 5(c) shows the slight asymmetry in the measured data which is not entirely accounted for by the standard model. The Leach model shows relatively close agreement with the data; however, it does not entirely account for the shape of the impedance curve in the high-frequency regime. The van-Maanen 1-group model has a better fit than the Leach model, but the best fit is observed with the van Maanen models with 3 or more groups.

Figure 6 shows the root mean squared (RMS) error of the mock data against the measured data for each model for the woofer (a) and the subwoofer (b). The RMS error does not improve significantly in either driver for van Maanen models with more than 3 groups. This trend is reflected in the model log-odds plots in Figure 7.

Figure 7 shows the model log-odds with respect to the standard model for the woofer (a) and the subwoofer (b). For the woofer, the log-odds peak at the 3-group van Maanen model, but for the subwoofer, the log-odds peak at the 5-group van Maanen model. For both drivers, each successive model shows a significant increase in log-odds up until the 3-group van Maanen model.

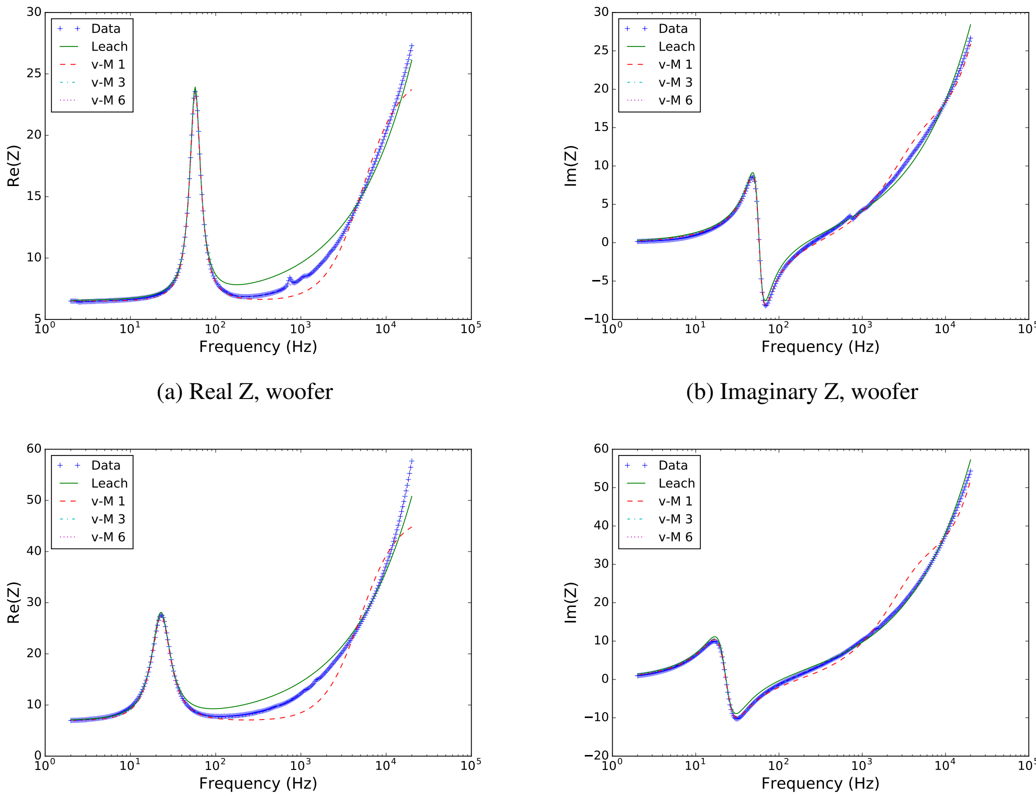

(a) Real Z, woofer

(b) Imaginary Z, woofer

(c) Real Z, subwoofer

(d) Imaginary Z, subwoofer

Figure 5. Mock data for selected models and measured data plotted against frequency.

DISCUSSION AND CONCLUSION

While a detailed decision-theoretical analysis is beyond the scope of this work, some general comments about making decisions using these results are given here. The log-odds for the models in the case of the woofer (Figure 7(a)), the mock data fit (Figure 5(a, b)), and the RMS error (Figure 6) suggest that the 3-group van Maanen model would be the best choice for designs involving this driver. The log-odds for the subwoofer (Figure 7(b)), however, give a less clear picture. If the cost function for the specific design task permits it, the 5-group van Maanen model would likely provide the greatest utility. If, however, the cost function penalizes additional groups, then the 3-group van Maanen model might provide the highest utility. The difference in the RMS error for the subwoofer between the 3-group and 5-group van Maanen models is nearly imperceptible, further supporting use of the 3-group model.

The slight difference in the peak model log-odds between the woofer and the subwoofer is likely explained by the physical differences between the two drivers. Specifically, the subwoofer necessarily has a larger magnetic structure, so more high-frequency loss is expected in the subwoofer. This increased loss means that the lossy inductive part of the impedance model has more of an effect on the model fit.

We have tested several other loudspeaker drivers in addition to those with results shown here, and preliminary results indicate that the van Maanen model (usually with 3 groups) consistently has the highest log-odds. These preliminary results lead us to expect consistent behavior among a diverse range of loudspeaker drivers.

Loudspeaker designers need accurate models to perform various related design tasks. We have presented several candidate loudspeaker driver models that account for the features of the loudspeaker impedance to varying degrees of success. The results, obtained through Bayesian model comparison using nested sampling on data obtained from testing of two loudspeaker drivers, show that the Leach model describes the loudspeaker impedance more accurately than the standard model, but the van Maanen model provides the best accuracy of the models tested.

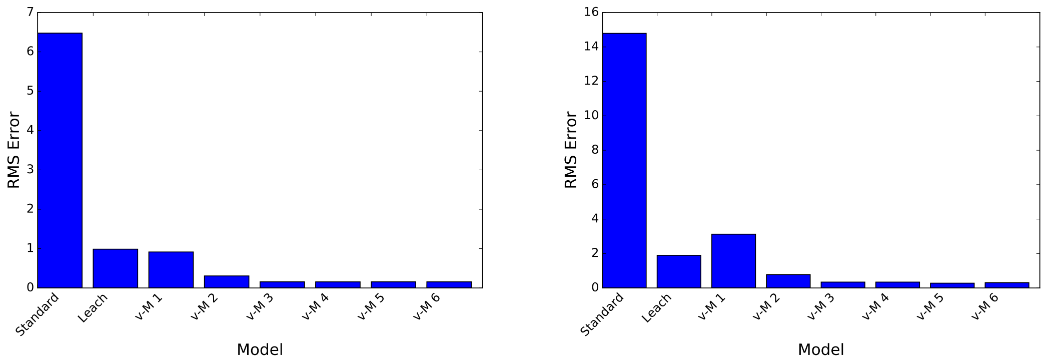

(a) Woofer (b) Subwoofer

Figure 6. RMS error for each model's MAP mock data against the measured data.

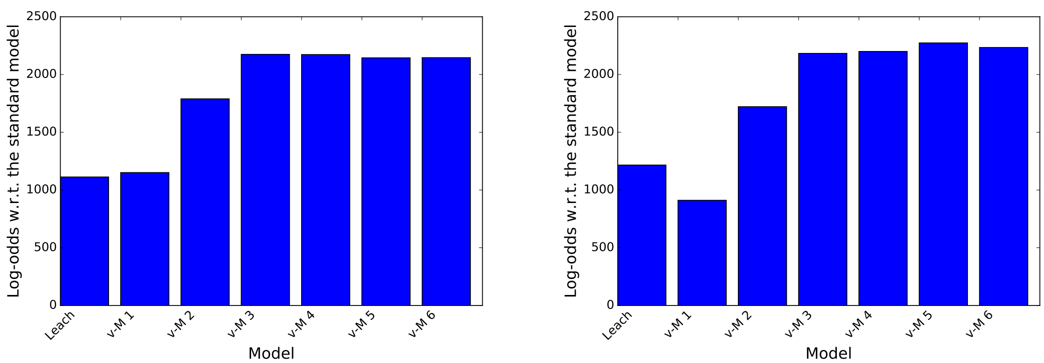

(a) Woofer (b) Subwoofer

Figure 7. Model log-odds with respect to the standard model for each of the tested drivers.

ACKNOWLEDGMENTS

We thank Wayne Prather for his assistance in performing measurements and the use of the Morel UW-1058c driver for testing. We also thank the National Center for Physical Acoustics (NCPA) for the use of their low-frequency anechoic chamber.

References

[1] W. M. Leach, Jr., Journal of the Audio Engineering Society **50**, 442–449June (2002).

[2] H. R. van Maanen and E. Zonneveld., "An extended model for impedance and compensation of electrodynamic loudspeaker units and an algorithm for their determination," in *Audio Engineering Society Convention 96* (1994).

[3] W. M. Leach, Jr., *Introduction to Electroacoustics & Audio Amplifier Design*, 4th ed. (Kendall Hunt, 2010).

[4] Iain, Loudspeaker cross section, https://commons.wikimedia.org/w/index.php?curid=1530955 (2006), accessed on 2016-07-07, licensed as CC-BY-SA-3.0-migrated.

[5] P. M. Goggans, L. Cao, and R. W. Henderson, "Assigning priors for parameters constrained to a simplex volume," in *AIP Conference Proceedings*, Vol. 1636, edited by R. K. Niven, B. Brewer, D. Paull, K. Shafi, and B. Stokes (2014), pp. 94–99.

[6] J. Skilling, Bayesian Analysis **1**, 833–859 (2006).